Journal of Orthopaedic Translation 31 (2021) 91–101

Contents lists available at ScienceDirect

Journal of Orthopaedic Translation

journal homepage: www.journals.elsevier.com/journal-of-orthopaedic-translation

A bio-inductive collagen scaffold that supports human primary tendon-derived cell growth for rotator cuff repair

Peilin Chen [a,h,1], Allan Wang [a,1], William Haynes [b,1], Euphemie Landao-Bassonga [a], Clair Lee [a], Rui Ruan [a], William Breidahl [c], Behzad Shiroud Heidari [d,e,f,g,h], Christopher A. Mitchell [a,h,*], Minghao Zheng [a,d,h,*]

[a] Centre for Orthopaedic Research, The UWA Medical School, The University of Western Australia, Crawley, WA, 6009, Australia
[b] Umhlanga Ridge Orthopaedic Centre, Suite 514 5th Floor, Gateway Private Hospital, 36 Aurora Drive, Umhlanga, 4320, South Africa
[c] Perth Radiological Clinic, Perth, Australia
[d] Perron Institute for Neurological and Translational Science, Perth, Western Australia, 6009, Australia
[e] Vascular Engineering Laboratory, Harry Perkins Institute of Medical Research, QEII Medical Centre, Nedlands, Australia
[f] UWA Centre for Medical Research, The University of Western Australia, Perth, Australia
[g] School of Engineering, The University of Western Australia, Perth, Australia
[h] Australian Research Council Centre for Personalised Therapeutics Technologies, Australia

ARTICLE INFO

Keywords:
Shoulder
Rotator cuff repair
Collagen-based scaffold
Cell culture
Tendon-derived cells

ABSTRACT

Background: Rotator Cuff (RC) tendon tearing is a common clinical problem and there is a high incidence of revision surgery due to re-tearing. In an effort to improve patient outcome and reduce surgical revision, scaffolds have been widely used for augmentation of RC repairs. However, little is known about how scaffolds support tendon stem cell growth or facilitate tendon regeneration. The purpose of this study is to evaluate the structural and biological properties of a bioactive collagen scaffold (BCS) with the potential to promote tendon repair. Additionally, we conducted a pilot clinical study to assess the safety and feasibility of using the BCS for repair of RC tears.

Methods: A series of physical, ultrastructural, molecular and *in vitro* tests determined the biocompatibility and teno-inductive properties of this BCS. In addition, a prospective case study of 18 patients with RC tendon tears (>20 mm in diameter) was performed in an open-label, single-arm study, involving either mini-open or arthroscopic surgical RC repair with the BCS. Clinical assessment of RC repair status was undertaken by MRI-imaging at baseline, 6 and 12 months and patient evaluated questionnaires were taken at baseline as well as 3, 6 & 12 months.

Results: The BCS consists of highly purified type-I collagen, in bundles of varying diameter, arranged in a higher order tri-laminar structure. BCS have minimal immunogenicity, being cell and essentially DNA-free as well as uniformly negative for the porcine α-Gal protein. BCS seeded with human primary tendon-derived cells and exposed to 6% uniaxial loading conditions *in vitro*, supported increased levels of growth and proliferation as well as up-regulating expression of tenocyte differentiation marker genes including TNMD, Ten-C, Mohawk and Collagen-1α1. To test the safety and feasibility of using the BCS for augmentation of RC repairs, we followed the IDEAL framework and conducted a first, open-label single arm prospective case series study of 18 patients. One patient was withdrawn from the study at 3 months due to wound infection unrelated to the BCS. The remaining 17 cases showed that the BCS is safe to be implanted. The patients reported encouraging improvements in functional outcomes (ASES, OSS and Constant-Murley scores), as well as quality of life assessments (AQoL) and a reduction in VAS pain scores. MRI assessment at 12 months revealed complete healing in 64.8% patients (11/17), 3 partial thickness re-tears (17.6%) and 3 full thickness re-tears (17.6%).

Conclusion: The BCS is composed of type-I collagen that is free of immunogenic proteins and supports tendon-derived cell growth under mechanical loading *in vitro*. This pilot study shows that it is safe and feasible to use BCS for RC argumentation and further controlled prospective studies are required to demonstrate its efficacy.

* Corresponding authors.
E-mail addresses: christopher.mitchell@uwa.edu.au (C.A. Mitchell), minghao.zheng@uwa.edu.au (M. Zheng).
[1] These authors contributed equally to this study

https://doi.org/10.1016/j.jot.2021.10.006
Received 22 July 2021; Received in revised form 20 October 2021; Accepted 22 October 2021

The Translational potential of this article: The results of this study indicate that this bioactive collagen scaffold has unique properties for supporting tendon growth and that it is non-immunogenic. The clinical study further confirms that the scaffold is a promising biological device for augment of human rotator cuff repairs.

1. Introduction

As much as 30% of the population report some degree of shoulder pain [1] and this proportion is expected to increase as the population ages. The most common cause of shoulder pain is rotator cuff (RC) tendinopathy and/or tear. Surgery is often recommended due to persistent pain, lifelong prevalence of clinical disability and the lack of an intrinsic capacity for the RC tendon to heal. Surgical repairs which anchor degenerative tendon(s) to the footprint of insertion are not always satisfactory. The rate of re-tearing after primary surgery or following revision is variable and can be as high as 94% [2–4].

The burden of RC disease and high incidence of re-tearing post-surgery have been powerful drivers for investigating the development of a wide range of biological [5] and synthetic [6] scaffolds that can potentially improve the functional outcome, reduce pain as well as decreasing the re-tear rate and requirement for revision surgery. A number of studies have demonstrated that surgical augmentation using scaffolds can reduce pain, result in higher patient satisfaction and improve function in comparison to non-augmented repairs [7,8]. A wide variety of synthetic materials have been developed for augmenting RC repairs, including polyester [9,10], polycarbonate/polyurethane [8], polyglycolic acid [11], polytetrafluoroethylene [12] and polypropylene [13]. These synthetic materials have shown improved biomechanical strength of the RC repair but there is a lack of evidence for their ability to aid tissue repair and regeneration of tendon structure. In contrast, biological scaffolds, composed of collagens derived from either xenograft or allograft tissue, may have the ability to support tendon-derived cell growth but generally lack biomechanical strength for augmentation of RC repair [6]. A range of sources has been used for processing or manufacture of biological scaffolds including allogenic skin [14–17], porcine dermis [7,18–23], porcine small intestinal sub-mucosa [24], bovine pericardium [13] as well as Achilles tendon [25,26]. There are some notable issues concerning the biocompatibility of biological scaffolds. Several RC scaffold repair materials contain significant amounts of foreign residual DNA [27,28] or the porcine xenoantigen galactose-α-1, 3-galactose (α-Gal) both of which have been associated with severe biological reactions resulting in their surgical excision [24,29–31]. Currently, there are concerns that xenograft and even allograft scaffolds may contain significant amounts of residual DNA and/or immunogenic proteins that compromise the efficacy and quality of scaffolds for RC repairs [6].

There is a clear clinical imperative for a user-friendly scaffold for use in augmenting RC repairs; that is, one which can be easily shaped to overlay the repair site, facilitates tendon regrowth by enhancing tendon cell growth and revascularization and if possible, provides additional biomechanical support during the early healing phase [32]. Here we report that BCS can be a user-friendly scaffold for augmenting RC repairs. We showed that BCS (manufactured by decellularization of porcine connective tissue [33]) is biocompatible, and is structurally unique, providing a highly-aligned tendon-like matrix that can respond to uniaxial loading for the growth and differentiation of primary human tendon-derived cells. In addition we demonstrated safety, patient and clinically-based outcome and quality of life measures in a series of 17 patients with RC tears who underwent either standard mini-open or arthroscopic RC repair augmented with BCS.

2. Materials and methods

Samples of BCS were prepared according to previously published methods [33] and the human tendon-derived cells [34] were provided by Orthocell for this study. The BCS was developed and validated for clinical use in tendon repair by Orthocell Pty Ltd, Australia, according to the code of Good Manufacturing Practice, and were cropped to various sizes according to the requirements of the individual experiment or clinical need. IDEAL guidelines for surgical innovation (idea and development stages; [35]) were used to govern the clinical pathway of the study.

2.1. Material characterization

We tested the BCS handling properties (including strength and suture retention properties) as well as its water retention capacity. The BCS thickness and water-absorbing characteristics was measured according to the method of Pallela [36]. Further details on the methodologies used to calculate strength measurement and suture retention properties of the BCS can be found in the supplementary methods section.

2.1.1. Determination of nuclear DNA content in BCS

To determine the potential immunogenicity from remnant nuclear material, the double stranded DNA content of connective tissue scaffold samples was determined using the Invitrogen Quant-IT™ according to the manufacturer's instructions. In brief, samples were prepared as 20 mg/ml working solutions and digested in collagenase (final concentration 10 mg/ml) for 18 h at 37 °C. Reaction buffer was added and 1, 10 or 20 μl of sample was added to the wells (triplicate repeats). A standard curve was generated to confirm linearity of DNA concentration determination produced by the assay ($R^2 = 0.999$). Absorbance was measured on a Molecular Devices Spectramax M5 plate reader at excitation of 480 nm and emission wavelength of 530 nm.

2.1.2. Determination of mitochondrial DNA content in BCS

Sample purifications and real-time PCR reactions were performed according to the manufacturer's instructions (Qiagen Mericon Pig kit; 292013). In brief, the PCR reaction consisted of 95 °C for 5 min followed by 95 °C for 15s, 60 °C for 23s and 72 °C for 10s (40 cycles). Total DNA content was assessed using a Nanodrop2000 (Thermo-Fisher, USA). Porcine connective tissue (starting material) and matched post-processing scaffold materials were obtained from 3 separate runs to determine batch variability. In each sample of (raw) starting material and scaffold, 3 separate internal replicates were conducted to determine intra sample variability. A 200 mg sample of each starting material was used for determination of mtDNA content, with 50ng/reaction for real-time PCR used as described in the manufacturer's instructions. An internal negative control (DNA diluent only) and positive control (porcine DNA = 120 ng/μl) were used to verify the PCR reaction.

2.1.3. Detection of cell nuclei remnants in BCS by histological analysis

Paraffin embedded sections of BCS samples were stained with haematoxylin and eosin (H & E) according to a standard protocol to detect cellular nuclei. Sections were flat mounted on glass slides and cover-slipped prior to imaging on a Zeiss light microscope at a range of objective magnifications.

2.1.4. Detection of immunogenic porcine α-Gal in BCS

Samples of raw material (prior to the decellularization process), positive control sample (porcine aortic valve) and BCS were embedded in OCT solution, frozen by immersion in iso-pentane cooled with liquid-N_2 and stored at −80 °C until use. Sections were cut on a cryomicrotome at 10 μm thickness and placed on sialinated glass slides. Sections were stained for α-Gal according to the manufacturer's (Invitrogen, USA) instructions, mounted with Diamond antifade mountant (Invitrogen, USA) and cover-slipped prior to imaging on a confocal microscope at a range of

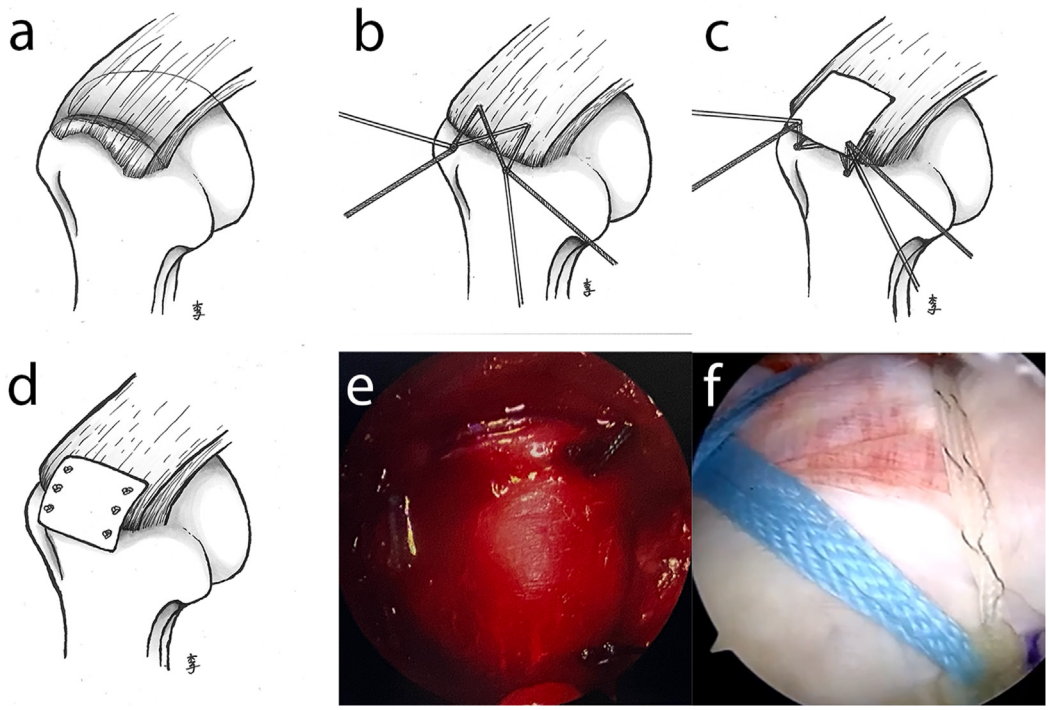

Fig. 1. *Schematic and intra-operative image of on-lay BCS repair of supraspinatus tendon.* **(a-c)** In either mini-open or arthroscopic surgical approaches, the footprint is prepared and sutures anchored. **(c)** A BCS patch (pre-measured to cover the repair site) was passed through the colour coded sutures onto the site of the footprint. **(d)** Sutures are fixed into the corners of the BCS patch. **(e)** Surgical repair of supraspinatus tendon with single-sheet BCS in place following mini-open or **(f)**arthroscopic surgery.

objective magnifications.

2.1.5. X-ray micro-tomography and scanning electron microscopy

BCS samples were processed for either X-ray microtomography or for ultrastructural analysis *via* scanning electron microscopy [33], according to our previously published methods. Detailed descriptions of these methods can be found in the supplementary methods and results section.

2.2. In vitro studies of BCS loaded with tendon-derived cells in a bioreactor

Primary human tendon-derived cells (from a total of 5 age-matched human tendon-biopsy samples; [34]) were obtained from Orthocell Ltd, cultured in 3D on BCS and exposed to either static or 6% uniaxial stretching conditions using our in-house bioreactor as previously described. Details of the cell culture and mechanical stimulation protocol, western blotting technique, cell population, proliferation and apoptosis assays, *Terminal deoxynucleotidyl transferase dUTP nick-end labelling* (TUNEL assay), Edu proliferation assay, Immunofluorescence labelling and confocal imaging as well as the quantitative PCR (qPCR) of tendon-specific genes are described in full in the accompanying supplementary methods and results section.

2.3. Prospective clinical case series

To test the feasibility for the use of BCS in augmentation of RC in surgery, we have followed the IDEAL framework of research innovation in surgery [35] and conducted a first open-label, single-arm pilot study in both mini-open and arthroscopic surgeries for repair of RC tears. All ethical considerations, including the study protocol, patient information, informed consent documents and other relevant documentation were approved by two independent Human Research Ethics Committees (St John of God Healthcare Human Research Ethics Committee [Perth, Western Australia] and Pharma-Ethics (Pty) Ltd, Registration No. 99/13868/07 [Pretoria, South Africa]) prior to study commencement. The study was also registered at ANZCTR (trial ID ACTRN12615001065583P).

2.3.1. Criteria for eligibility

Participants were at least 40 years old and presented with symptomatic full-thickness supraspinatus ± infraspinatus tear >20 mm as verified by MRI, ultrasound imaging or during surgical repair. The exclusion criteria for this study included evidence of other clinically significant pathology of the affected shoulder, subscapularis tear requiring surgical repair, prior shoulder surgery or fracture, active infection or systemic pathology (e.g. inflammatory joint disease, HIV, poorly controlled diabetes and neoplastic disorders), metabolic bone disorder, neuromuscular disease of the affected arm, professional athletes and workers compensation cases.

2.4. Surgery

All surgical procedures were performed by two surgeons (AW & WH). Short-term post-operative care included immobilisation of the affected shoulder in an abduction sling for six weeks followed by application of a standardised post-surgical rehabilitation program [37].

2.4.1. Mini-open approach

In the lateral decubitus position, glenohumeral and subacromial arthroscopic evaluation was performed. A calibrated probe was used to confirm a full-thickness supraspinatus tear measuring greater than 20 mm in antero-posterior extent. The subacromial bursa, cuff tendon edge and greater tuberosity footprint were debrided with a full radius arthroscopic resector. An acromioplasty was performed in all cases. Concomitant acromioclavicular joint arthropathy was treated by arthroscopic excision of the lateral end of clavicle and lesions of the long head of biceps tendon were treated by biceps tenotomy.

The supraspinatus tendon tear was repaired with a double row suture bridge technique (Wang 2015), and a full repair was achieved in all cases.

A 3 cm deltoid splitting mid-lateral surgical approach was made to the rotator cuff repair site. The BCS patch was cut to the appropriate size, such that the medial edge of the patch was medial to the medial suture knots, and the lateral edge of the patch was overlapping the lateral edge of the repaired cuff tendon by 5 mm. Typically the patch was 25 mm–30 mm in AP dimension and 20 mm in medial-lateral dimension. The rough side of the patch was placed against the bursal surface of the native tendon. When hydrated, the patch adhered and conformed closely to the underlying cuff tendon. The patch was sutured to the cuff tendon with 2:0 Ethibond or 2:0 PDS simple sutures and the lateral edge of the patch was fixed to the greater tuberosity with the lateral row anchor sutures (Fig. 1).

2.4.2. Arthroscopic technique

The patient was placed in the beach chair position with the operated arm positioned in abduction and forward flexion. Glenohumeral and subacromial arthroscopy was performed and the full thickness supraspinatus tendon tear was measured with the calibrated probe. Eligibility for study inclusion was confirmed. Concomitant pathology was treated appropriately. The bursa and cuff tear and greater tuberosity were debrided. An acromioplasty was performed in all cases.

A double row arthroscopic cuff repair was performed with two Healicoil anchors (5.5 mm Smith and Nephew) as medial row anchors and incorporating both sutures and tapes. The sutures and tapes were passed through the tendon, 8–12 mm medial to the free edge of the torn tendon. The sutures were tied to reduce the cuff down onto the greater tuberosity. The BCS patch was measured to cover the repair. Stay colour-coded sutures were placed into the corners of the patch, allowing for easy manipulation within the subacromial space. The patch was folded twice allowing passage into the subacromial space. The stay sutures were retrieved sequentially though percutaneous posterosuperior, anterosuperior, posteroinferior and anteroinferior portals. The patch was gently manipulated into position by pulling on the stay sutures. The tapes were then retrieved in a suture bridge configuration and secured using two knotless anchors (Footprint 5.5 mm; Smith & Nephew) creating the lateral footprint. The patch was evenly distributed over the rotator cuff repair (Fig. 1). The portals were closed using subcutaneous 3-0 Vicryl, Steri-Strips and a Primapore dressing applied.

2.4.3. Safety endpoints

Adverse events related to study treatment or procedures were recorded and assessed. These included any systemic or local immune/inflammatory reaction or other systemic adverse event related to the study treatment. In addition surgical or significant medical intervention required as a result of treatment failure was considered a safety endpoint.

2.4.4. Outcome assessment

At baseline, 3, 6 and 12 months post-treatment an assessment of symptoms and disability was determined by OSS [38], ASES [39] and Constant-Murley Score [40], in addition to quality of life measurement by AQoL [41]. Alleviation of pain was measured as an improvement in the VAS pain score [42] at 1, 3, 6 and 12 months post-treatment.

The MRI assessments were used to evaluate the safety and efficacy of implanted BCS and re-tear rate. All patients underwent pre-operative as well as 6 and 12 month post-operative MRI scans and were examined to determine the success of rotator cuff repair and the biocompatibility/potential benefit of the BCS. High resolution MRI scans were performed on a Phillips 3T Achieva platform (Best, The Netherlands). Standard proton-density and T2 fat suppressed images were obtained in the sagittal and coronal images with a FOV of 14 cm, slice thickness of 3–3.5 mm, and a minimum 512 × 512 matrix for the T2 fat suppressed images increasing into the range of 700–900 for the proton density images.

2.5. Statistical methods

All values for pre-clinical assessment data are expressed as mean ± SEM, unless otherwise noted. A 2-tailed Student's t test and 1-way ANOVA, followed by Tukey post hoc test (GraphPad 5.0; GraphPad Software, La Jolla, CA, USA), were used for determining the statistical significance ($p < 0.05$) in the 2-group and multi-group comparisons, respectively. Clinical data were entered into Excel spreadsheet and exported to SPSS (v26) for generation of descriptive statistics and testing of the null hypothesis that there is no difference between the means for outcome measures or patient demographics at each time point. Omnibus testing was performed using the repeated measures ANOVA (parametric) or Friedman's ANOVA (non-parametric measures). Post hoc pairwise testing was conducted using Bonferroni correction and restricted to baseline *versus* time-point pair only. All tests were two-sided with $\alpha = 0.05$.

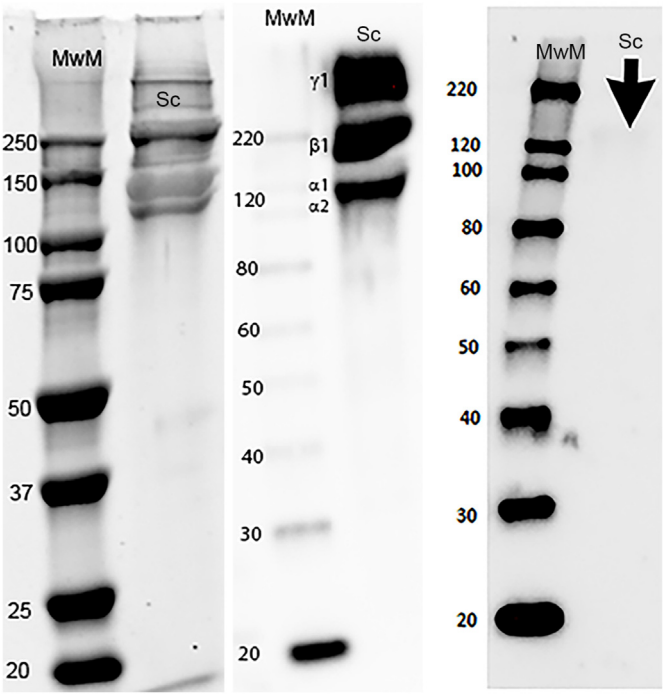

Fig. 2. – *Protein and collagen-I/III western blotting of BCS.* Following coomassie blue labelling of collagen scaffold extracts, several bands with molecular weights higher than 120 kDa were seen **(left panel).** Staining with a collagen type-I specific antibody revealed 3 distinctive bands **(middle panel)** corresponding to the α1/α2, β1 and χ1 chains respectively. Staining with a collagen III specific antibody **(right panel)** revealed weak immunoreactivity (arrow) corresponding to a molecular weight of approximately 160 kDa. M_wM = molecular weight marker; Sc = collagen scaffold sample.

3. Results

3.1. Material characterization

3.1.1. Handling properties

BCS are flat sheets that maintain their shape. The thickness of single BCS sheets used for material characterisation analysis of water retention are 358 ± 87 μm (range 253–511; n = 4). The BCS are able to retain 478 ± 26% (n = 6) of their initial weight in water. These physical properties allow the accurate conformation of hydrated BCS with underlying surface topology (Fig. 1e and f). The maximum tensile strength of 6 individual BCS membranes (247 ± 20 μm thickness) was calculated for both dry (9.78 ± 1.25 MPa) and wet samples (2.95 ± 0.40 MPa). The suture retention forces were determined in duplicates from 3 samples each (345 ± 87 μm thickness) tested with either 2:0 monofilament was 7.34 ± 1.22N (n = 3; range 6.63 – 8.76N) or 3:0 monofilament was 9.37 ± 1.64N (n = 3; range 8.42 – 11.26N). Following hydration BCS are flexible and

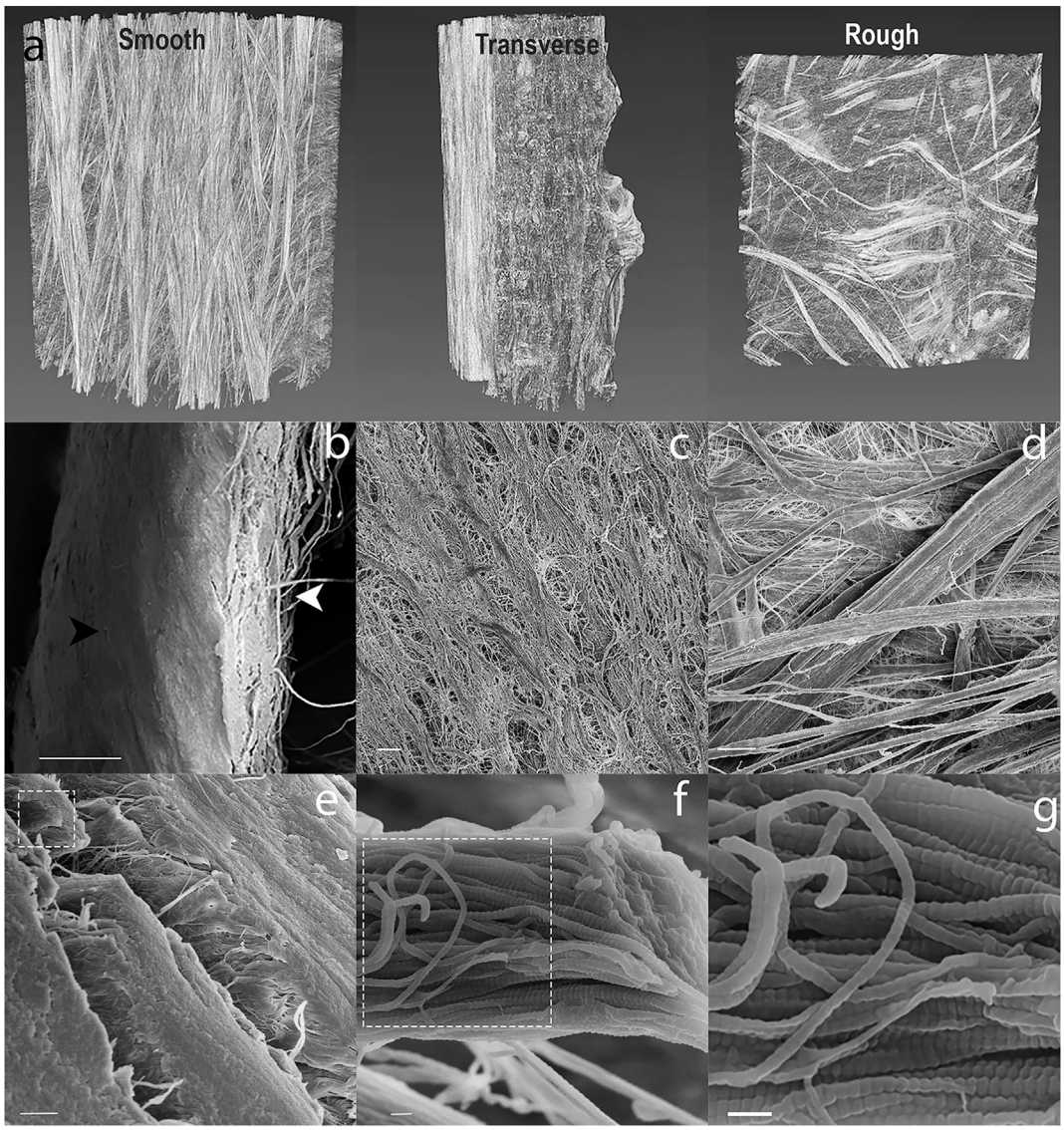

Fig. 3. - *Ultrastructural imaging of BCS with x-ray computed microtomography and SEM.* (a) X-ray microtomography rendered image of the smooth surface of the BCS showing regularly aligned bundles of collagen. In the transverse image (middle panel) peripherally located smooth and rough surfaces surround a less dense core. On the rough side (right panel) collagen fibres are more loosely and randomly arranged. In a low power electron microscopic image of a transverse sectioned BCS (b) surface features of the smooth side (black arrowhead) and rough side (white arrowhead) are conspicuous. The BCS smooth side demonstrates loosely and irregularly arranged collagen bundles with sub-micron sized gaps (c). On the rough side, randomly oriented fibre bundles are discerned (d). Adjacent to the smooth surface in this transverse section (e), numerous densely packed fibre bundles are observed. (f) A higher magnification (from the boxed area in e) reveals tightly packed individual type-I collagen fibrils within a bundle. In this high power image (from the boxed area in f) characteristic D-banding of collagen type-I (g) is clearly evident. Bar = 100mm (b), 10mm (c), 1mm (d), 100nm (e), 200nm (f & g).

can be folded into multiple layers to increase the strength (data not shown).

3.1.2. *BCS are composed of type-I collagen*

We first conducted coomassie blue protein staining of the BCS and revealed a discrete series of high molecular weight bands ranging in size from 120 to 350 kDa (Fig. 2; left panel). After probing with porcine collagen I specific antibody, 3 bands corresponding to α1/α2 (120 kDa), β1 (200 kDa) and γ1 (350 kDa) forms of collagen IαI were detected (Fig. 2; middle panel). Re-probing the membrane with a collagen III-specific antibody revealed a very weakly positive band at 140 kDa (Fig. 2; right panel). These results confirm that BCS are composed almost exclusively of type-I collagen.

To characterise 3D structure, axial alignment and fibrillary composition of type I collagen, we undertook both x-ray computed micro-tomography and SEM analysis of the BCS. Cross-sectional x-ray computed micro-tomographic analysis, revealed that the BCS are layered fibrous structures (Fig. 3a) with highly aligned, tightly bundled anisotropic fibres on one side (smooth; Fig. 3a middle panel) adjacent to a porous core of loosely arranged collagen I and bounded by a more open and less ordered isotropic structure (rough) on the other (Fig. 3a; right panel). SEM analysis confirmed that the smooth surface (Fig. 3b) contains thin flattened bundles of collagen fibres separated by less dense regions with sub-micron size gaps in between (Fig. 3c). The rough surface contains both single collagen fibrils and flattened fibre bundles that are loosely arranged and irregularly oriented (Fig. 3d). Adjacent to the smooth side of the scaffolds (Fig. 3a and b), high power SEM reveals anisotropic and tightly packed bundles (Fig. 3e), with characteristic type-1 collagen fibrils (Fig. 3f) with a typical collagen type-I D-banding morphology and ~65 nm periodicity.

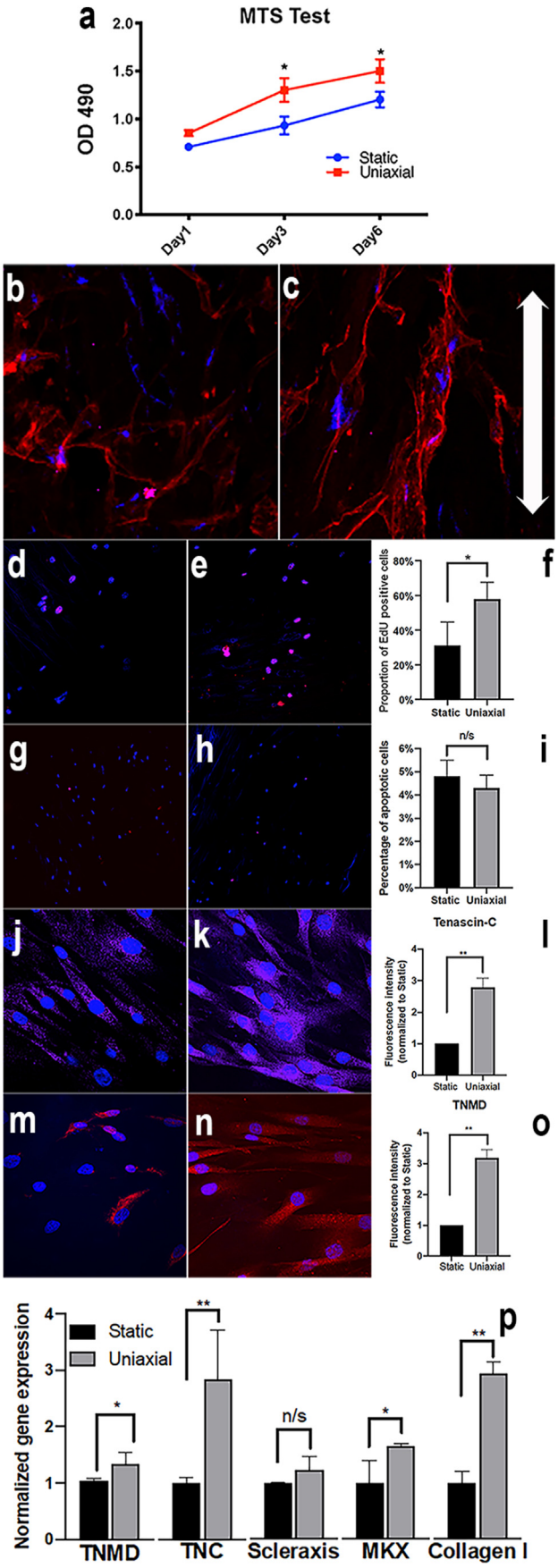

(caption on next column)

Fig. 4. – *Growth, proliferation and differentiation of tendon-derived cells on BCS.* MTS cell viability assay of primary human tendon-derived cells grown on collagen scaffold material **(a)**. At both 4 & 6 days after seeding, cell viability was increased in the 6% loaded group compared to the static control (0%; $p < 0.05$). Primary human tendon-derived cells seeded in static conditions were randomly oriented on the matrix **(b)**, whereas those subjected to 6% uniaxial loading were more closely aligned with the direction of force **(arrows: c)**. Labelling with EdU in the static **(d)** compared to the 6% uniaxial loaded group **(e)** revealed a statistically significant increase (*$p < 0.05$) in cell proliferation **(f)**. TUNEL labelling of tendon-derived cells grown on collagen scaffolds exposed to static **(g)** or 6% loading **(h)** conditions showed there were similar numbers of apoptotic cells **(NS, *p > 0.05; i)**. Primary human tendon-derived cells grown under static conditions showed relatively low levels of tenomodulin **(j)** which was increased in the 6% loading condition **(k)** some 3-fold **(**p < 0.01; l)**. Similarly, tenascin-C was expressed in static loaded primary tenocyte cultures **(m)** although this was increased in 6% loading conditions **(n)** up to 2.5-fold **(*p < 0.05; o)**. mRNA levels **(p)** for tendon-specific genes were significantly increased following 6% loading in primary tenocyte cultures for tenomodulin ($p < 0.05$), tenascin-C ($p < 0.01$), mohawk ($p < 0.05$) and collagen I ($p < 0.01$), although there were no significant differences in the levels of scleraxis (NS, $p > 0.05$). *$p < 0.05$, **$p < 0.01$, TNMD = tenomodulin, MKX = mohawk. Bar = 20 μm in g, h, j & k; 50 μm in b, c, e & f.

3.1.3. BCS are free of DNA and α-Gal

We have previously reported that several collagen scaffolds that were widely used for RC repairs contain cellular/DNA components [28] and these contaminants may underlie the severe immune rejection reactions following implantation, such as those described for the Restore scaffold [30,31,43]. To determine if BCS contains nuclear and mitochondrial DNA and α-Gal, we performed histology, immunohistochemical detection (for α-Gal) an industry standard (PicoGreen) spectrophotometric method and a real-time PCR-based mitochondrial DNA assay to assure BCS are free of DNA and α-Gal content.

The results showed that the raw material for BCS contains a uniform pattern of eosinophilic fibre distribution with sparsely distributed basophilic nuclei characteristic of loose connective tissue (Suppl. Figure 1a). In contrast, BCS contains no nuclear material (Suppl. Figure 1b), consistent with removal of cellular removal from the scaffolds during processing. To further test the nuclear DNA content, we used the PicoGreen spectrophotometric method [44] and the result showed that the nuclear DNA content of BCS was below the detection limit of the assay or <0.05 ng DNA/mg material.

We next used real-time PCR (Mericon mtDNA detection kit) to define traceable mitochondrial DNA (mtDNA) content levels in BCS. The result showed that starting raw materials of BCS contain mtDNA at a level of 112 ng/mg, at 80 bp bands corresponding to the cytochrome C target. In contrast, BCS contains minimum traceable porcine DNA at a level less than 0.32 ng/mg (Suppl. Figure 2). To summarize, these results show that BCS contain almost undetectable levels of nuclear and mitochondrial DNA. The manufacturing process enabled a 350-fold reduction in DNA content compared to the raw material.

To examine for the presence of α-Gal in BCS, we used porcine aorta as positive control and compared the positivity of α-Gal in both the starting raw material and final BCS implant. The result showed the highly immunogenic α-Gal expression in positive control porcine aorta (Suppl. Fig 3a) and lower levels of immuno-reactivity of α-Gal expression in starting raw material (Suppl. Fig. 3b), whereas BCS were uniformly negative (Suppl. Figure 3c).

3.2. BCS induces tendon-derived cell growth and differentiation under uniaxial-loading in a bioreactor

We next hypothesised that human tendon-derived cells seeded on BCS *in vitro* respond to mechanical loading by increasing cell growth, aligning along fibres orienting with the direction of force transmission and express increased levels of tendon-specific differentiation markers. Using the MTS assay we observed that cell viability on both static and 6%

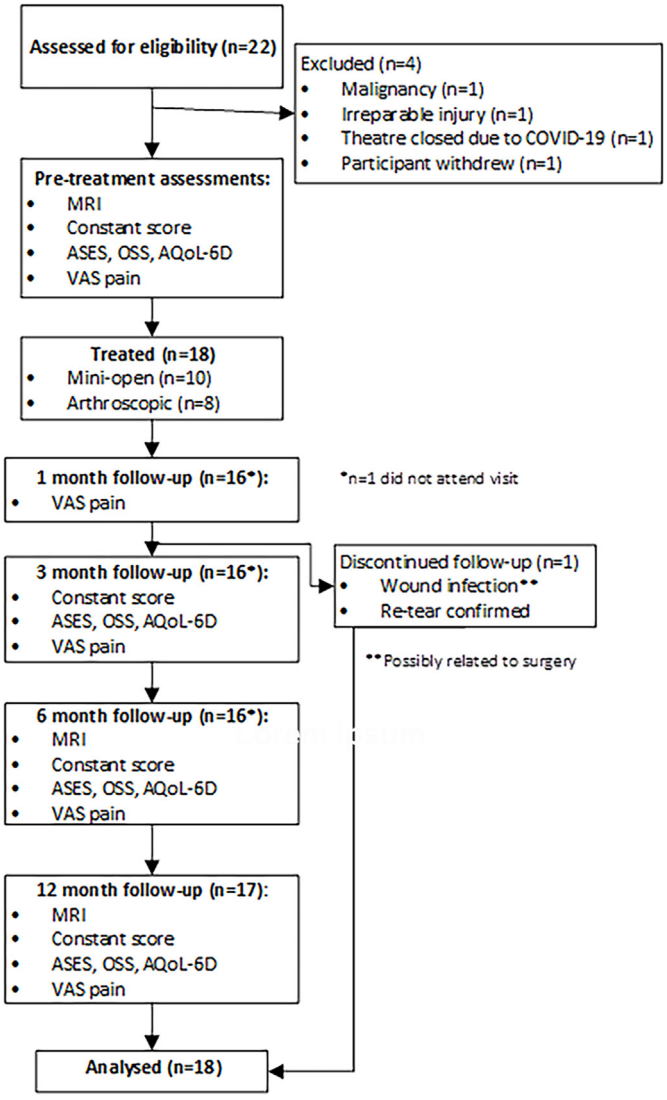

Fig. 5. CONSORT (Consolidated Standard of Reporting Trials) flowchart for patients enrolled on the BCS RC surgical repair study (combined mini-open and arthroscopic approaches). MRI = magnetic resonance imaging; Constant Score = Constant-Murley outcome questionnaire; ASES = American Shoulder and Elbow Surgeons questionnaire; OSS = Oxford Shoulder Score questionnaire; AQoL-6D = Adjusted Quality of Life questionnaire; VAS = Visual Analogue Score questionnaire.

mechanically loaded BCS increased during the 1–6 days of uniaxial-loading in a bioreactor (Fig. 4a). In the 6% uniaxially-loaded BCS at days 4 & 6 a significant increase in $O.D._{490}$ was observed in comparison to statically loaded cell scaffolds (*$p < 0.05$). Cells were bipolar, rounded and more randomly aligned in static cultures (Fig. 4b), whereas in 6% loading conditions they were highly aligned along the direction of force and exhibited an extended, spindle shaped morphology (Fig. 4c). In order to assess tenocyte proliferation, cells were labelled with the s-phase specific marker EdU. Static cultures showed significantly less nuclear specific labelling than those exposed to 6% loading (Fig. 4d–f; $p < 0.05$). As the total cell population is also regulated by the proportion of cell death, we assessed TUNEL immunofluorescence labelling of nuclei on BCS from both static (Fig. 4g) and uniaxially loaded samples (Fig. 4h). There was no statistically significant difference in the numbers of TUNEL-labelled cells between groups (Fig. 4i), indicating that the cell viability increases in response to 6% mechanical loading (Fig. 4a) are largely due to the increased cell proliferation (Fig. 4f). Together these results indicate that BCS transmits the forces generated during uniaxial loading to increase tenocyte growth in bioreactor.

There is considerable debate concerning the identification of tenocyte precursors or mature tenocytes, although a number of markers are recognised and widely used [45]. These include the helix-loop-helix transcription factor scleraxis (Scx), along with the TALE family atypical Iriquois-like homeodomain protein mohawk (Mkx) which are amongst the earliest markers of tenocyte differentiation. These transcription factors are responsible for regulation of tenocyte specific structural proteins including the glycoprotein tenomodulin (Tnm), the cross-linking protein tenascin-C (Ten-C) and the main structural collagens including Col-1α1. In order to determine if BCS can transmit mechanical loading to human tendon-derived cells, inducing tenocyte differentiation and tendon-matrix protein production, we immunostained samples with tnm and 10-C, or quantified cDNA from these cultured cells for tnm, scx, mkx, 10-C or col-1α1. Immunolabelling for tenascin-C (Fig. 4j-l) and tenomodulin (Fig. 4m–o), revealed that both these tendon specific proteins were raised in cultures exposed to 6% uniaxial loading. When mRNA retrieved from cultures was analysed by reverse transcriptase-PCR for tendon-specific gene expression, tenomodulin (*$p < 0.05$), tenascin-C (**$p < 0.01$), mohawk (*$p < 0.05$) and collagen type-I (**$p < 0.01$) levels were all significantly increased in 6% uniaxial loaded cultures (Fig. 4p). The cDNA levels for scleraxis were not significantly different between static and 6% uniaxially loaded tenocyte cultures (NS; $p > 0.05$). Together these results showed that the BCS induces tenocyte growth and differentiation *in vitro*.

3.3. Prospective clinical case series study

3.3.1. Patient demographics and RC status

We recruited a total of 18 patients (including 2 women; Fig. 5), with a mean SEM age of 61.9 ± 10.1 (range 46.3–80.8 years). The duration of pre-operative pain in the affected shoulder was 43.9 ± 61.1 months (mean ± SEM; range 0.5–240 months) with 16 of the injuries being the result of trauma and 2 due to degenerative changes. Five were former smokers. There were no patients enrolled in the study who were lost to follow up. The antero-posterior mean tendon tear size at baseline in this series of patients was 26.2 ± 3.4 mm (mean ± SEM).

3.3.2. Complications

One patient had a wound infection at 9 weeks post-surgery (Fig. 5) with the causative organism being identified as a *Corynebacterium* sp. This patient responded well to *i.v.* Levofloxacin, prior to arthroscopic washout and debridement. In the clinical judgement of the surgeon this adverse event of infection was unrelated to the BCS but possibly related to the procedure. Following debridement and 5 days of oral Levofloxacin, the patients' recovery was uneventful. Due to this adverse event it was deemed to not be in the best interests of the patient to continue with study follow-up.

3.3.3. Clinical outcomes

In order to determine whether the mini-open (Suppl. Table 1a) or arthroscopic (Suppl. Table 1b) surgical approaches could be considered as one cohort (Suppl. Table 2) for the purposes of this study, baseline characteristics were compared with respect to age, duration of symptoms and outcome measures (Constant score, OSS, ASES, AQoL and VAS pain score). The null hypothesis (i.e. there are no significant differences between these characteristics when comparing the mini-open and arthroscopic approaches) was tested for each parameter using two-sided Student's T tests with $\alpha = 0.05$. All comparisons between groups were found to be not statistically significant, indicating that the groups could be merged and considered as a single cohort for the purposes of analysis (Suppl. Table 2).

Functional outcome assessment revealed progressive improvements in scores compared to baseline following BCS augmentation RC surgery (Supplementary Table 2). All shoulder outcome measures were significantly improved compared to baseline at 12 months: ASES (Fig. 6a; 61.1

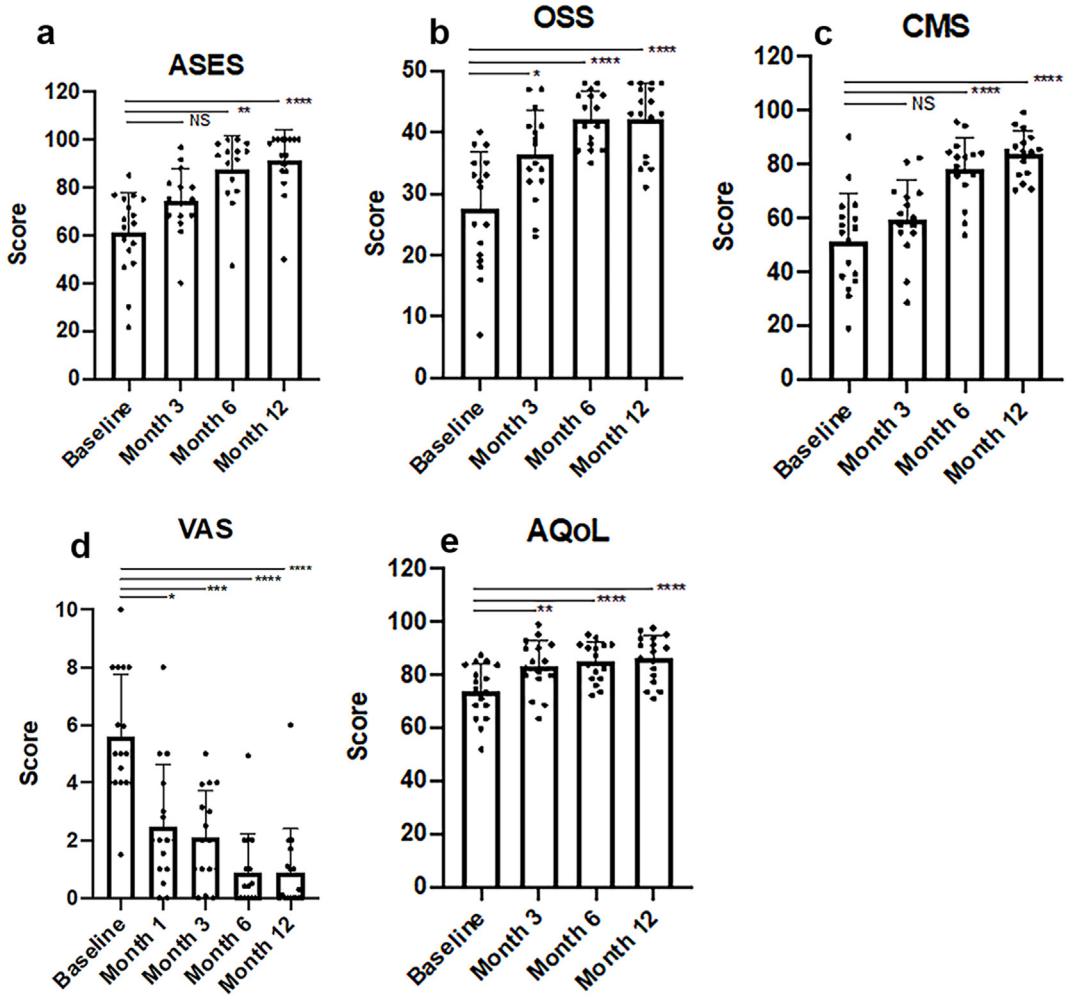

Fig. 6. Bar graphs of clinical and patient reported outcome scores following RC surgery augmented with BCS. ASES (a), OSS (b), Constant-Murley (c), VAS-pain (d) and AQoL (e). Individual points within each bar represent single patient scores. Data is represented as mean ± SEM. NS = not significant ($p > 0.05$); *$p < 0.05$; **$p < 0.01$; ***$p < 0.005$; ****$p < 0.001$ (ANOVA).

± 17.0 [range 21.7–85.0] vs 91.0 ± 13.3 [range 50–100]; $p < 0.001$), OSS (Fig. 6b; 27.5 ± 9.3 [range 7–40] vs 42.2 ± 5.8 [31–48]; $p < 0.001$) and Constant-Murley (Fig. 6c; 51.4 ± 17.7 [range 18.8–90] vs 83.6 ± 8.6 [range 70.0–99.1]; $p < 0.001$). The degree of shoulder pain in this series of patients (VAS pain scores) at baseline compared to 12 months were also significantly improved (Fig. 6d; 5.6 ± 2.1 [range 1.5–10] vs 0.9 ± 1.5; range 0–6; $p < 0.001$) as were the quality of life indicator AQoL scores (Fig. 6e; 73.7 ± 10.2 [range 51.9–87.3] vs 86.2 ± 8.6 [range 70.9–97.5]; $p < 0.001$). None of these patients experienced any adverse events or the requirement for revision surgery.

MRI assessment of 17 patients at 12 months revealed complete healing in 64.8% patients (11/17), 3 partial thickness re-tears (17.6%) and 3 full thickness re-tears (17.6%). Representative baseline T2w fat suppressed MRI images (Fig. 7a and c) from patients proceeding to either mini open (Fig. 7e) or arthroscopic (Fig. 7f) surgical procedures, show full thickness supraspinatus detachment from the RC anatomical footprint prior to repair. At 6 months following surgical repair there is evidence of BCS path signal and there is no longer a fluid filled defect at the footprint (Fig. 7b and e) in comparison to baseline, with the repaired tendon containing mildly increased signal intensity. MRI imaging at 12 months (Fig. 7c and f) indicates successful healing of the full thickness supraspinatus tendon tears.

4. Discussion

Collagen-based devices have the potential to facilitate tendon regeneration. A parallel-aligned matrix is important as it can respond to uniaxial loading and permits the ingrowth, proliferation and differentiation of locally situated tendon-derived cells. It has been shown that non-aligned collagen-based devices derived from skin (such as GraftJacket and Permacol), in which the structure does not mimic native tendon matrix, display histological evidence of a chronic fibro-inflammatory response and contribute to a failure in clinical outcomes [46]. Here we show that BCS contains highly aligned type-I collagen fibres in matrix without immunogenic materials such as α-Gal and DNA, and maintains its bio-inductive properties supporting tendinogenesis *ex vivo*. The type-1 collagen matrix has a unique tri-laminar structure. Its 3D morphology is characterised by loose and randomly arranged fibrils on the "rough" side, adjacent to a porous core and bounded by dense anisotropically aligned fibre bundles on the "smooth" side. This BCS enables the support of tendon-derived cell growth and differentiation in a dynamic mechanical environment. Tendon-derived cells seeded on BCS are viable, proliferate and produce tendon-specific transcription factors and matrix proteins. Furthermore, BCS seeded with tendon-derived cells and subjected to 6% uniaxial-loading, increase their growth and tendon-specific gene expression. This data supports the conclusion that an interplay between BCS structural properties and mechanical stimulation is able to induce host tendon cell differentiation and matrix production. Our pilot

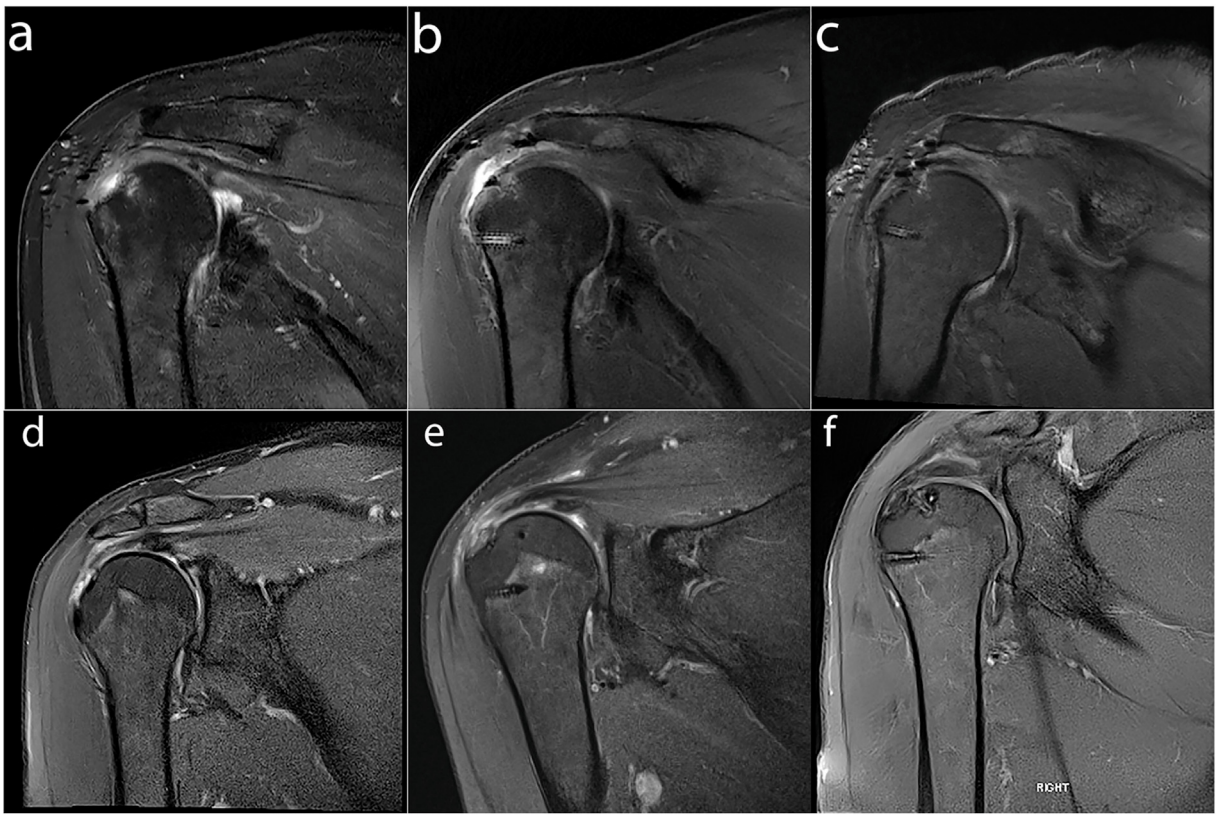

Fig. 7. T1-weighted coronal magnetic resonance images from patients at baseline (a & d), 6-months (b & e) and 12 months (c & f) following either mini-open (a–c) or arthroscopic repair (d–f) of the RC with a BCS. (a) Supraspinatus full thickness tear extending to infraspinatus with associated tendinopathy. (b) Supraspinatus tendon displayed intermediate signal intensity of BCS patch. No fluid filled defect at the footprint was seen. (c) Supraspinatus tendon repair intact with no evidence of re-tear. (d) Supraspinatus full thickness tear extends to the footprint. (e) The region of supraspinatus and infraspinatus tendons display intermediate signal intensity, reflecting the repair process of BCS. (f) Supraspinatus full thickness tear resolved with no evidence of re-tear.

case-series clinical study confirms that the BCS is safe and may be promising for use in RC tear repairs. All of the 17 patients who underwent surgical argumentation with either the mini-open or arthroscopy procedure (including those who completed the clinician/patient outcome measures) have achieved relatively good clinical outcomes without any adverse events or the requirement for revision surgery.

Essential criteria for biological devices that are intended for RC tendon repair are its surgical handling properties, mechanical soundness and that it is non-immunogenic [32]. We have shown that BCS absorbs water/tissue fluids, conform to the shape of the repair site, are biocompatible and demonstrate no evidence of an inflammatory response. The BCS hold at least 4 times its weight in water and have a porous architecture, which permits retention of blood components/bone marrow stem cells released during the reconstruction procedure which are postulated to aid in the regeneration and healing of the RC tendon [47]. Currently, reports on the clinical usage of collagen-based medical devices used in RC repair state that they are not intended to perform a mechanical support role [48,49] but there is an essential requirement for suture retention during surgery. While a single sheet of BCS do not achieve the required retention strength for biomechanical support of the RC tendon, this preliminary study in humans has shown that the suture retention and material strength is sufficient for overlay of the RC surgical repair.

Xenobiotic and allogeneic collagen-based graft materials for surgical augmentation of RC repairs have been shown to cause severe localized inflammation, tissue rejection and significant rates of re-tearing [29,43,50]. Several scaffold types proposed as augmentation devices for human soft tissue, including TissueMend, Restore and Graftjacket were found to contain significant amounts of DNA and/or cellular material capable of inducing an immune reaction and severe inflammatory phenomena [28,49]. One of these, Graftjacket is a collagen I based material derived from human cadaveric skin, has been used for over 800,000 augmentations of RC repairs by 2011. This material has also been reported to contain allogeneic material that may underlie the reports of adverse events [46]. Failure to remove the immunogenic elements of remnant DNA and non-collagenous impurities (such as lipids and non-structural proteins) in these collagen-I enriched scaffolds used for RC repairs, is largely attributable to the manufacturing process and the source of starting material [28]. For this reason we evaluated the efficiency of the proprietary based procedure for cellular and immunogenic material removal from the BCS. We used a range of methodologies for detection of residual DNA, including the industry standard PicoGreen assay [44], detection of basophilic nuclear staining with haematoxylin staining, as well as detection of porcine mitochondrial DNA using real-time PCR [51]. BCS are essentially free of cellular material. The residual DNA levels we detected were well below those described for other materials [27]. This *in vitro* data, coupled with the results of the pilot clinical study, are strongly supportive of the conclusion that BCS have a below-threshold level of contaminants and do not induce a detectable immune response in human patients. In addition, we have shown that BCS are also able to transmit the mechanical loading *in vitro* which is a process that is necessary for successful tendon repair. Consistent with previous studies [52], we showed that the growth of human primary tendon-derived cells on BCS subjected to 6% uniaxial load is accompanied by increased cell viability, directed cell alignment, an increase in S-phase DNA synthesis and induction of tendon matrix production.

This pilot human safety study showed that BCS is safe and feasible for use in patients during mini-open or arthroscopic RC repair. We showed that BCS can be sutured and anchored to the bursal surface of the tendon with the potential to facilitate regenerative tissue repair. Functional

outcomes scores were all significantly improved in this pilot cohort at 12 months in comparison to baseline, including ASES, OSS, Constant-Murley, AQoL and VAS Pain measurements. These results are encouraging, as at 12 months the overall healing rate for BCS augmented repairs was 70% and importantly there were no referrals for revision surgery. This bodes well for long-term outcome in this series of patients, as the 12-month outcome is predictive of long-term functional recovery after RC repairs [53]. Re-tearing is common finding following RC repairs. Although we also observed re-tears after surgery, our results are consistent with those reported in a systematic review of retear rates in scaffold augmented rotator cuff repairs [54]. There are a number of risk factors reported in meta-analyses of outcomes of rotator cuff surgery that can contribute to a higher rate of re-tearing. These include age [55], size of the initial tear [56], level of post-surgical activity [57], prior corticosteroid administration [58], low HDL levels [59] as well as co-existent shoulder pathology or a fibro-inflammatory genotype of the repaired tendon [60] and further studies will be required to determine the causes of re-tearing following augmentation of RC repairs with BCS.

The limitations of the clinical pilot study are the small number of patients and the lack of a prospective control group (i.e. those not receiving BCS augmentation). An appropriately powered case-matched, randomized controlled study would be necessary to assess the efficacy of the BCS and to determine whether the various concomitant surgical procedures (e.g. acromial decompression and biceps tenodesis/tenotomy) impact the potential improvements in strength, function and shoulder pain as a result of augmentation. The current study was performed in accordance with the IDEAL framework and was specifically designed for intermediate tears with diameters >20 mm [61]. Further studies would also need to be conducted to determine if the BCS can be used to augment RC repairs in large or massive antero-posterior tears [47,54,62].

5. Conclusion

The BCS is a teno-inductive/teno-conductive matrix for growth of primary human tendon-derived cells *in vitro*. Furthermore, the results of this pilot case-series indicates that BCS is safe and feasible for use in the treatment of intermediate size RC tears.

Funding

This work is supported by Australian Research Council Industrial Transformation Training Centre for Personalised Therapeutics Technologies grant (IC170100016) and a research grant from Orthocell.

Declaration of competing interest

MHZ and AW are consultants to Orthocell Ltd and hold stock in the company. CL is the Director of Research and Development at Orthocell Ltd. All the other authors declare that they have no competing financial interests.

Acknowledgements

The authors wish to express their gratitude to Dr Tak Cheng and Mr Luke Hanrahan for assistance with data collection and collation as well as Dr Anne Bonser for manuscript editing.

Appendix A. Supplementary data

Supplementary data to this article can be found online at https://doi.org/10.1016/j.jot.2021.10.006.

References

[1] Makela M, Heliovaara M, Sainio P, Knekt P, Impivaara O, Aromaa A. Shoulder joint impairment among Finns aged 30 years or over: prevalence, risk factors and co-morbidity. Rheumatology 1999;38(7):656–62.
[2] Cole BJ, McCarty 3rd LP, Kang RW, Alford W, Lewis PB, Hayden JK. Arthroscopic rotator cuff repair: prospective functional outcome and repair integrity at minimum 2-year follow-up. J Shoulder Elbow Surg 2007;16(5):579–85.
[3] Klepps S, Bishop J, Lin J, Cahlon O, Strauss A, Hayes P, et al. Prospective evaluation of the effect of rotator cuff integrity on the outcome of open rotator cuff repairs. Am J Sports Med 2004;32(7):1716–22.
[4] McElvany MD, McGoldrick E, Gee AO, Neradilek MB, Matsen 3rd FA. Rotator cuff repair: published evidence on factors associated with repair integrity and clinical outcome. Am J Sports Med 2015;43(2):491–500.
[5] Nho SJ, Delos D, Yadav H, Pensak M, Romeo AA, Warren RF, et al. Biomechanical and biologic augmentation for the treatment of massive rotator cuff tears. Am J Sports Med 2010;38(3):619–29.
[6] Hakimi O, Mouthuy PA, Carr A. Synthetic and degradable patches: an emerging solution for rotator cuff repair. Int J Exp Pathol 2013;94(4):287–92.
[7] Badhe SP, Lawrence TM, Smith FD, Lunn PG. An assessment of porcine dermal xenograft as an augmentation graft in the treatment of extensive rotator cuff tears. J Shoulder Elbow Surg 2008;17(1 Suppl):35S–9S.
[8] Encalada-Diaz I, Cole BJ, Macgillivray JD, Ruiz-Suarez M, Kercher JS, Friel NA, et al. Rotator cuff repair augmentation using a novel polycarbonate polyurethane patch: preliminary results at 12 months' follow-up. J Shoulder Elbow Surg 2011;20(5):788–94.
[9] Nada AN, Debnath UK, Robinson DA, Jordan C. Treatment of massive rotator-cuff tears with a polyester ligament (Dacron) augmentation: clinical outcome. J Bone Joint Surg Br 2010;92(10):1397–402.
[10] Ozaki J, Fujimoto S, Masuhara K, Tamai S, Yoshimoto S. Reconstruction of chronic massive rotator cuff tears with synthetic materials. Clin Orthop Relat Res 1986;(202):173–83.
[11] Mochizuki Y, Ochi M. Clinical results of arthroscopic polyglycolic acid sheet patch graft for irreparable rotator cuff tears. Asia Pac J Sports Med Arthrosc Rehabil Technol 2015;2(1):31–5.
[12] Hirooka A, Yoneda M, Wakaitani S, Isaka Y, Hayashida K, Fukushima S, et al. Augmentation with a Gore-Tex patch for repair of large rotator cuff tears that cannot be sutured. J Orthop Sci 2002;7(4):451–6.
[13] Ciampi P, Scotti C, Nonis A, Vitali M, Di Serio C, Peretti GM, et al. The benefit of synthetic versus biological patch augmentation in the repair of posterosuperior massive rotator cuff tears: a 3-year follow-up study. Am J Sports Med 2014;42(5):1169–75.
[14] Barber FA, Burns JP, Deutsch A, Labbe MR, Litchfield RB. A prospective, randomized evaluation of acellular human dermal matrix augmentation for arthroscopic rotator cuff repair. Arthroscopy 2012;28(1):8–15.
[15] Bond JL, Dopirak RM, Higgins J, Burns J, Snyder SJ. Arthroscopic replacement of massive, irreparable rotator cuff tears using a GraftJacket allograft: technique and preliminary results. Arthroscopy 2008;24(4):403–409 e1.
[16] Laskovski J, Abrams J, Bogdanovska A, Taliwal N, Taylor M, Fisher M. Arthroscopic rotator cuff repair with allograft augmentation: making it simple. Arthrosc Tech 2019;8(6):e597–603.
[17] Pandey R, Tafazal S, Shyamsundar S, Modi A, Singh HP. Outcome of partial repair of massive rotator cuff tears with and without human tissue allograft bridging repair. Shoulder Elbow 2017;9(1):23–30.
[18] Castagna A, Cesari E, Di Matteo B, Osimani M, Garofalo R, Kon E, et al. Porcine dermal xenograft as augmentation in the treatment of large rotator cuff tears: clinical and magnetic resonance results at 2-year follow-up. Joints 2018;6(3):135–40.
[19] Consigliere P, Polyzois I, Sarkhel T, Gupta R, Levy O, Narvani AA. Preliminary results of a consecutive series of large & massive rotator cuff tears treated with arthroscopic rotator cuff repairs augmented with extracellular matrix. Arch Bone Jt Surg 2017;5(1):14–21.
[20] Flury M, Rickenbacher D, Jung C, Schneider MM, Endell D, Audige L. Porcine dermis patch augmentation of supraspinatus tendon repairs: a pilot study assessing tendon integrity and shoulder function 2 Years after arthroscopic repair in patients aged 60 Years or older. Arthroscopy 2018;34(1):24–37.
[21] Gupta AK, Hug K, Boggess B, Gavigan M, Toth AP. Massive or 2-tendon rotator cuff tears in active patients with minimal glenohumeral arthritis: clinical and radiographic outcomes of reconstruction using dermal tissue matrix xenograft. Am J Sports Med 2013;41(4):872–9.
[22] Lederman ES, Toth AP, Nicholson GP, Nowinski RJ, Bal GK, Williams GR, et al. A prospective, multicenter study to evaluate clinical and radiographic outcomes in primary rotator cuff repair reinforced with a xenograft dermal matrix. J Shoulder Elbow Surg 2016;25(12):1961–70.
[23] Muench LN, Kia C, Jerliu A, Williams AA, Berthold DP, Cote MP, et al. Clinical outcomes following biologically enhanced patch augmentation repair as a salvage procedure for revision massive rotator cuff tears. Arthroscopy 2020;36(6):1542–51.
[24] Bryant D, Holtby R, Willits K, Litchfield R, Drosdowech D, Spouge A, et al. A randomized clinical trial to compare the effectiveness of rotator cuff repair with or without augmentation using porcine small intestine submucosa for patients with moderate to large rotator cuff tears: a pilot study. J Shoulder Elbow Surg 2016;25(10):1623–33.
[25] Bokor DJ, Sonnabend D, Deady L, Cass B, Young A, Van Kampen C, et al. Evidence of healing of partial-thickness rotator cuff tears following arthroscopic augmentation with a collagen implant: a 2-year MRI follow-up. Muscles Ligaments Tendons J 2016;6(1):16–25.

[26] Thon SG, O'Malley 2nd L, O'Brien MJ, Savoie 3rd FH. Evaluation of healing rates and safety with a bioinductive collagen patch for large and massive rotator cuff tears: 2-year safety and clinical outcomes. Am J Sports Med 2019;47(8):1901–8.
[27] Gilbert TW, Freund JM, Badylak SF. Quantification of DNA in biologic scaffold materials. J Surg Res 2009;152(1):135–9.
[28] Zheng MH, Chen J, Kirilak Y, Willers C, Xu J, Wood D. Porcine small intestine submucosa (SIS) is not an acellular collagenous matrix and contains porcine DNA: possible implications in human implantation. J Biomed Mater Res B Appl Biomater 2005;73(1):61–7.
[29] Malcarney HL, Bonar F, Murrell GA. Early inflammatory reaction after rotator cuff repair with a porcine small intestine submucosal implant: a report of 4 cases. Am J Sports Med 2005;33(6):907–11.
[30] Phipatanakul WP, Petersen SA. Porcine small intestine submucosa xenograft augmentation in repair of massive rotator cuff tears. Am J Orthop (Belle Mead NJ) 2009;38(11):572–5.
[31] Walton JR, Bowman NK, Khatib Y, Linklater J, Murrell GA. Restore orthobiologic implant: not recommended for augmentation of rotator cuff repairs. J Bone Joint Surg Am 2007;89(4):786–91.
[32] Chainani A, Little D. Current status of tissue-engineered scaffolds for rotator cuff repair. Tech Orthop 2016;31(2):91–7.
[33] Allan B, Ruan R, Landao-Bassonga E, Gillman N, Wang T, Gao J, et al. Collagen membrane for guided bone regeneration in dental and orthopedic applications. Tissue Eng Part A; 2020.
[34] Wang A, Breidahl W, Mackie KE, Lin Z, Qin A, Chen J, et al. Autologous tenocyte injection for the treatment of severe, chronic resistant lateral epicondylitis: a pilot study. Am J Sports Med 2013;41(12):2925–32.
[35] McCulloch P, Cook JA, Altman DG, Heneghan C, Diener MK, Group I. IDEAL framework for surgical innovation 1: the idea and development stages. BMJ 2013; 346:f3012.
[36] Pallela R, Venkatesan J, Janapala VR, Kim SK. Biophysicochemical evaluation of chitosan-hydroxyapatite-marine sponge collagen composite for bone tissue engineering. J Biomed Mater Res A 2012;100(2):486–95.
[37] Wang A, McCann P, Colliver J, Koh E, Ackland T, Joss B, et al. Do postoperative platelet-rich plasma injections accelerate early tendon healing and functional recovery after arthroscopic supraspinatus repair? A randomized controlled trial. Am J Sports Med 2015;43(6):1430–7.
[38] Dawson J, Fitzpatrick R, Carr A. Questionnaire on the perceptions of patients about shoulder surgery. J Bone Joint Surg Br 1996;78(4):593–600.
[39] Michener LA, McClure PW, Sennett BJ. American shoulder and elbow surgeons standardized shoulder assessment form, patient self-report section: reliability, validity, and responsiveness. J Shoulder Elbow Surg 2002;11(6):587–94.
[40] Constant CR, Murley AH. A clinical method of functional assessment of the shoulder. Clin Orthop Relat Res 1987;214:160–4.
[41] Wylie JD, Beckmann JT, Granger E, Tashjian RZ. Functional outcomes assessment in shoulder surgery. World J Orthop 2014;5(5):623–33.
[42] Tashjian RZ, Deloach J, Porucznik CA, Powell AP. Minimal clinically important differences (MCID) and patient acceptable symptomatic state (PASS) for visual analog scales (VAS) measuring pain in patients treated for rotator cuff disease. J Shoulder Elbow Surg 2009;18(6):927–32.
[43] Iannotti JP, Codsi MJ, Kwon YW, Derwin K, Ciccone J, Brems JJ. Porcine small intestine submucosa augmentation of surgical repair of chronic two-tendon rotator cuff tears. A randomized, controlled trial. J Bone Joint Surg Am 2006;88(6): 1238–44.
[44] Ahn SJ, Costa J, Emanuel JR. PicoGreen quantitation of DNA: effective evaluation of samples pre- or post-PCR. Nucleic Acids Res 1996;24(13):2623–5.
[45] Li Y, Wu T, Liu S. Identification and distinction of tenocytes and tendon-derived stem cells. Front Cell Dev Biol 2021;9:629515.
[46] Rashid MS, Smith RDJ, Nagra N, Wheway K, Watkins B, Snelling S, et al. Rotator cuff repair with biological graft augmentation causes adverse tissue outcomes. Acta Orthop 2020;91(6):782–8.
[47] Goldenberg BT, Lacheta L, Dekker TJ, Spratt JD, Nolte PC, Millett PJ. Biologics to improve healing in large and massive rotator cuff tears: a critical review. Orthop Res Rev 2020;12:151–60.
[48] Barber FA, Herbert MA, Coons DA. Tendon augmentation grafts: biomechanical failure loads and failure patterns. Arthroscopy 2006;22(5):534–8.
[49] Derwin KA, Baker AR, Spragg RK, Leigh DR, Iannotti JP. Commercial extracellular matrix scaffolds for rotator cuff tendon repair. Biomechanical, biochemical, and cellular properties. J Bone Joint Surg Am 2006;88(12):2665–72.
[50] Sclamberg SG, Tibone JE, Itamura JM, Kasraeian S. Six-month magnetic resonance imaging follow-up of large and massive rotator cuff repairs reinforced with porcine small intestinal submucosa. J Shoulder Elbow Surg 2004;13(5):538–41.
[51] Al-Kahtani HA, Ismail EA, Ahmed MA. Pork detection in binary meat mixtures and some commercial food products using conventional and real-time PCR techniques. Food Chem 2017;219:54–60 [English].
[52] Chen P, Chen Z, Mitchell C, Gao J, Chen L, Wang A, et al. Intramuscular injection of Botox causes tendon atrophy by induction of senescence of tendon-derived stem cells. Stem Cell Res Ther 2021;12(1):38.
[53] Collin P, Kempf JF, Mole D, Meyer N, Agout C, Saffarini M, et al. Ten-Year multicenter clinical and MRI evaluation of isolated supraspinatus repairs. J Bone Joint Surg Am 2017;99(16):1355–64.
[54] D'Ambrosi R, Ragone V, Comaschi G, Usuelli FG, Ursino N. Retears and complication rates after arthroscopic rotator cuff repair with scaffolds: a systematic review. Cell Tissue Bank 2019;20(1):1–10.
[55] Khazzam M, Sager B, Box HN, Wallace SB. The effect of age on risk of retear after rotator cuff repair: a systematic review and meta-analysis. JSES Int 2020;4(3): 625–31.
[56] Lobo-Escolar L, Ramazzini-Castro R, Codina-Grano D, Lobo E, Minguell-Monyart J, Ardevol J. Risk factors for symptomatic retears after arthroscopic repair of full-thickness rotator cuff tears. J Shoulder Elbow Surg 2021;30(1):27–33.
[57] Saltzman BM, Zuke WA, Go B, Mascarenhas R, Verma NN, Cole BJ, et al. Does early motion lead to a higher failure rate or better outcomes after arthroscopic rotator cuff repair? A systematic review of overlapping meta-analyses. J Shoulder Elbow Surg 2017;26(9):1681–91.
[58] Cimino AM, Veazey GC, McMurtrie JT, Isbell J, Arguello AM, Brabston EW, et al. Corticosteroid injections may increase retear and revision rates of rotator cuff repair: a systematic review. Arthroscopy 2020;36(8):2334–41.
[59] Park HB, Gwark JY, Kwack BH, Jung J. Hypo-high-density lipoproteinemia is associated with preoperative tear size and with postoperative retear in large to massive rotator cuff tears. Arthroscopy 2020;36(8):2071–9.
[60] Eager JM, Warrender WJ, Deusenbery CB, Jamgochian G, Singh A, Abboud JA, et al. Distinct gene expression profile in patients with poor postoperative outcomes after rotator cuff repair: a case-control study. Am J Sports Med 2021;49(10): 2760–70.
[61] Sugaya H, Maeda K, Matsuki K, Moriishi J. Functional and structural outcome after arthroscopic full-thickness rotator cuff repair: single-row versus dual-row fixation. Arthroscopy 2005;21(11):1307–16.
[62] Thangarajah T, Pendegrass CJ, Shahbazi S, Lambert S, Alexander S, Blunn GW. Augmentation of rotator cuff repair with soft tissue scaffolds. Orthop J Sports Med 2015;3(6). 2325967115587495.